Post-Buckling Behaviour of Ring-Stiffened Cylinders Under Lateral Pressure

S.S. Seleim, J. Roorda
University of Waterloo, Dept. of Civil Engineering, Waterloo, Ontario N2L 3G1, Canada

Abstract

The post-buckling behaviour of ring-stiffened cylinders subjected to lateral pressure and failing in either the general or shell instability modes is studied. Theoretical analysis was carried out using the energy method. Suitable non-linear terms of the buckling displacement were retained in the total potential energy expression. A sinusoidal buckling shape was assumed and initial imperfections were assumed to have the same shape as the failure buckling mode. The theoretical results were compared with the results of ten machined ring-stiffened cylinders tested under lateral pressure. The analysis showed the post-buckling behaviour to be stable symmetric for both modes. The experimental results indicate a neutral or a slightly stable behaviour for both modes.

Method, Assumptions and Results

In general, a ring-stiffened cylinder subjected to lateral pressure may buckle into the general (Fig. 1) or the shell (Fig. 2) instability modes. The size and number of rings as well as the overall dimensions of the cylinder influence the buckling mode.

This paper presents the results of a theoretical and experimental study of the post-buckling behaviour of ring-stiffened cylinders failing by one of the above mentioned instability modes. The theory used is a non-linear post-buckling analysis based on the earlier linear buckling theory of Kendrick [1], which employs the strain energy method. Under lateral pressure, the stiffened cylinder undergoes a uniform radial contraction and a uniform longitudinal elongation. Hence, it is important to consider second order terms in the longitudinal and circumferential strain displacement relationships. However, since shear strains are zero just prior to buckling, it is reasonable for shear strains to consider first order terms only. The extensional strain energy expression contained up to and including fourth order terms of the buckling displacements, while higher order terms of the buckling displacements were ignored in the bending strain energy expression because bending strains prior to buckling are very small. The following sinusoidal buckling shape was assumed:

$$\begin{aligned} u &= A \cos n\theta . \cos \frac{m\pi x}{L} \\ v &= B \sin n\theta . \sin \frac{m\pi x}{L} \\ w &= C \cos n\theta . \sin \frac{m\pi x}{L} \end{aligned} \qquad (1)$$

Initial imperfection in the form of initial out-of-roundness were assumed to have the same shape as the buckling displacement as follows:

$$w_o = C_o \cos n\theta . \sin \frac{m\pi x}{L} \qquad (2)$$

The variables m and n are the number of longitudinal and circumferential waves, respectively. The critical pressure and the corresponding values of m_{cr} and n_{cr} were obtained through a minimization process of the total strain energy expression with respect to the variables m and n. With reference to Figs. 1 and 2, it can be seen that the variable m_{cr} is equal to 1 and N+1 for the general and shell instability modes, respectively, where N is the number of stiffening rings.

The analysis showed the post-buckling behaviour to be stable symmetric (see Fig. 3).

The analysis was used to study the post-buckling behaviour of ten aluminum ring-stiffened cylinders tested under lateral pressure. Five of the ten cylinders failed by the shell instability mode, while the others failed by the general instability mode. All the cylinders had the same diameter, wall thickness and overall length. The size and number of rings were varied from one cylinder to another so that the weight of all the cylinders remained at 6.57 kg (14.5 lb). The Batdorf parameter Z for the ten stiffened cylinders ranged between 9 and 180. Circularity contours shown in Figs. 4 and 5 were obtained using a number of direct current displacement transducers. The experimental values of the amplitudes of the critical buckling mode were obtained by analyzing the circularity contours into its basic components using Fourier expansion. Detailed description of the experimental set-up and testing procedure can be found in [2].

Sample plots of pressure versus buckling amplitudes are shown in Fig. 6 for a stiffened cylinder which failed by general instability and in Fig. 7 for another cylinder which failed by shell instability. In Figs. 6 and 7, the solid curves represent the equilibrium paths obtained from the analysis. Each individual point, *, corresponds to a single equilibrium position obtained from the experiments, i.e., corresponds to the amplitude of the critical buckling mode obtained from the circularity contours using Fourier expansion, as mentioned above.

For the two buckling modes, the analysis shows a stable symmetric post-buckling behaviour with a relatively more stable behaviour for the ease of shell instability mode. The experimental results indicate a neutral or a slightly stable post-buckling behaviour for both the shell and the general instability modes. It is worth to mention that three of the five cylinders which failed by shell instability did so due to rupture at the end ring at pressures slightly higher than the critical pressure obtained from the analysis. This could indicate a reserve of post-buckling strength in the case of the shell instability mode.

References

[1] Kendrick, S., "The Buckling Under External Pressure of Ring Stiffened Circular Cylinders", Trans. Royal Institute of Naval Architects, Vol. 107, 1965, pp. 139-156.

[2] Seleim, S.S. and Roorda, J., "Buckling of Ring Stiffened Cylinders, Experimental Study", SMD Report no. 195, University of Waterloo.

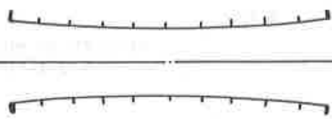

(b)

General Instability Mode

(GIM)

FIG. 1

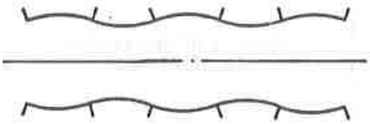

(c)

Shell Instability Mode

(SIM)

FIG. 2

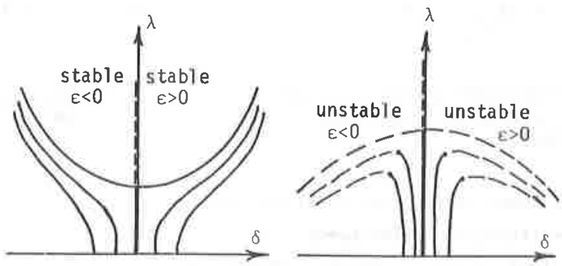

FIG. 3

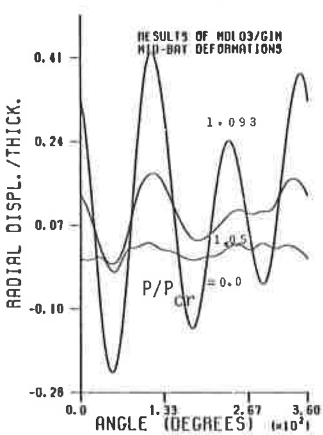

FIG. 4

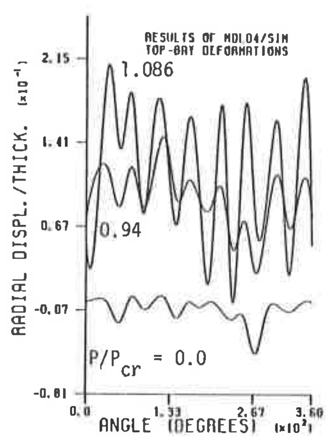

FIG. 5

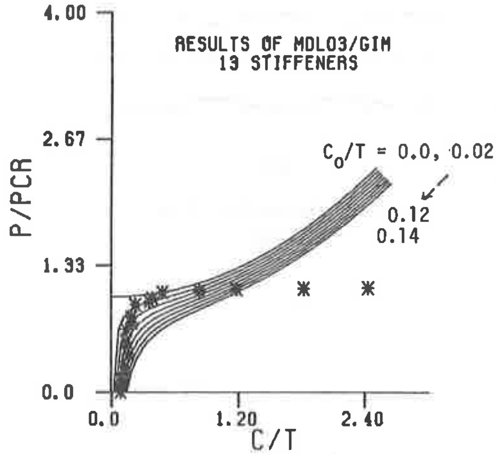

FIG. 6 - Post-Buckling Behaviour of the General Instability Mode.

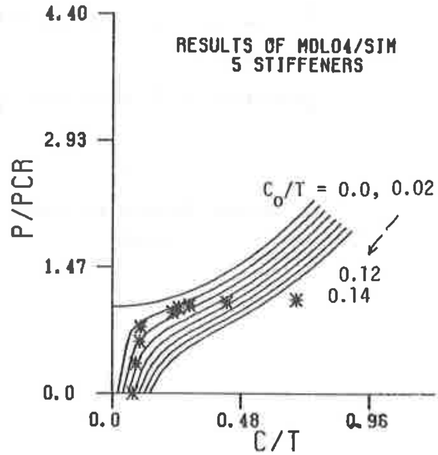

FIG. 7 - Post-Buckling Behaviour of the Shell Instability Mode.

P/PCR: Pressure/Theoretical Buckling Pressure.

C/T: Amplitude/Shell Thickness

C_0/T: Initial Imperfection/Shell Thickness.